Control of a Solar Furnace using Active Cooling*

Bertinho A. Costa[1], João M. Lemos[2] and Emmanuel Guillot[3]

Abstract— This paper explores a control architecture for a solar furnace that uses active cooling to improve the temperature reference tracking during the decreasing phase of the reference. This is done in conjunction with the command of the shutter that adjusts the incident power and compensates sun power variability due to weather conditions. The controller uses exact linerization coupled with a PI controller to handle model parameter uncertainty. Off-line identification is employed to characterize the temperature dynamics, this is used to avoid online adaptation mechanisms that may cause stability problems during the controller startup, that may melt the material sample. Experimental results obtained from the plant in closed loop control using active cooling are presented.

Index Terms— Solar Furnace, Non-linear Dynamics, Off-line Identification, Active Cooling.

I. INTRODUCTION

The study of material aging processes is usually carry out using temperature cycling stress tests. In this research field, solar furnaces are used to apply concentrated solar energy on samples to obtain high temperature stress tests. The PROMES Solar Energy Laboratory at Odeillo, southern France (fig. 1), and the Plataforma Solar de Almeria (southern Spain) [1], are two sites where concentrated solar energy are used in several applications such as to develop material stress tests.

In this process the temperature dynamics is nonlinear, since it depends on the fourth power temperature term and on the nonlinear static function of the shutter, that is employed to adjust the incident power. Depending on the purpose of the experiment, a temperature reference is selected and must be followed with accuracy. From previous studies, the tracking of a decreasing reference using only the shutter aperture may not be adequate because the natural power losses by convection and by radiation are not adequate. In this situation, when the shutter is closed, active cooling must be employed.

A solar furnace comprises a heliostat that tracks the sun and guides the solar energy to a parabolic mirror that concentrates energy on a focus. The energy applied on the material sample is adjusted by commanding the shutter aperture. Figure 2 shows the $900W$ solar furnace at PROMES used in the tests with a SiC sample at the testing table on the

[1] INESC-ID/IST, University of Lisbon, Rua Alves Redol, 9 1000-029, Portugal bac@inesc-id.pt

[2]INESC-ID/IST, University of Lisbon, Rua Alves Redol, 9 1000-029, Portugal jlml@inesc-id.pt

[3]CNRS-PROMES, 7 rue du Four Solaire, 66120 Font Romeu Odeillo, France emmanuel.guillot@promes.cnrs.fr

Fig. 1. PROMES laboratory at Odeillo, southern France, showing the 1MW parabolic mirror (north part of the building) and the heliostat field. Smaller size solar furnaces are located in the building at its southern part.

Fig. 2. Visualization the $900W$ solar furnace at PROMES with a SiC sample on the testing table. The air flow nozzle for active cooling is above (away) the sample. The sun light is guided by a heliostat at the ground level to the parabolic mirror that concentrates the light. A pyrometer located near the parabolic mirror measures the temperature of the sample.

focus. Light strips on the parabolic mirror depend on the shutter aperture. The air flow nozzle for active cooling is above (away) the sample.

The temperature dynamics of a sample has a nonlinear behavior [1], depends on the material properties, on the sample size, on the power losses by radiation and by convection and on the energy absorption.

Uncertainty on the material thermodynamic properties and the energy transfer between the sample and the environment affect the characterization of the temperature model. Solar power fluctuations induced by the presence of clouds, if not compensated, also affect the operation of the solar furnaces and the results of temperature stress experiments.
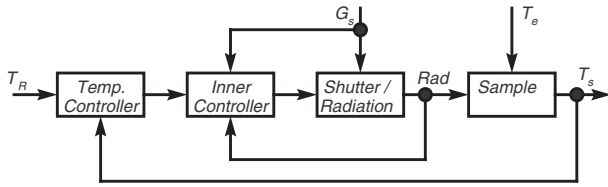
Fig. 3. Control system architecture for the solar furnace. The temperature controller generates a reference power value for the inner controller. The inner controller compensates the nonlinear static function of the shutter and the variability of the sun power.

Several works were developed to address the temperature control in solar furnaces as [1]. The nonlinear model is linearized and a linear model is identified that depends on the temperature level.

An enhanced temperature control architecture was proposed in [2], the aim being to explore a cascade control architecture with two loops to decouple the shutter nonlinearity from the temperature dynamics. In [3] a predictive adaptive controller was used in parallel with a PI controller to control the temperature of the sample. The aim was to use the adaptive controller to improve the performance in situations where the PI controller was not well tuned. In this approach however, the online adaptation may cause stability problems. In [4] optimal control is evaluated in the control of a solar furnace.

In this paper the parameters of the nonlinear model are identified offline to avoid the identification of several local linear models, an approach first evaluated in [5]. Disturbance rejection in solar furnaces is handle in [6], feedback linearization with GPC control applied to solar furnaces is explored in [7] and [8]. In [9] predictive control with integral action was applied to a solar furnace at PROMES with success using off-line identification.

In this framework, off-line model identification is employed to characterize the temperature dynamics. The model identified includes the contribution of the losses by convection and by radiation and the incident power that is regulated by the shutter. The effect of active cooling can be modelled with a term that is similar to the term that represents losses by natural convection. But in the present work active cooling is considered as a disturbance, meaning that it must be compensated by adjusting the incident power. The control system architecture is illustrated in the figure 3, where the temperature controller generates a reference power value for the inner controller. The inner controller controls the aperture of the shutter, compensates the nonlinear static function of the shutter and the variability of the sun power.

From the results obtained, it is concluded that the approach followed can be applied in practice to improve the operation of solar furnaces.

This paper is organized as follows, after this introduction, section II describes the model of a solar furnace. Section III describes the methodology used to off-line model identification using data collected from the process. The control law

using exact linearization coupled with a PI is described in the section IV. The results obtained from the the plant operating in closed loop with the application of active cooling are presented in section V. The conclusion are presented in the last section.

II. SOLAR FURNACE MODEL

The solar furnace model comprises two dynamic models: a dynamic model that describes the interactions between the concentrated solar energy and the temperature of the sample, and the model that describes the behaviour of the shutter. These models are presented hereafter.

A. Shutter model

The shutter operates in closed loop using a servo mechanism. The shutter has a dynamics much faster than the thermal model subsystem, and therefore only the static function of the shutter is considered,

$$s_{fs}(u_s(t)) = 1 - \frac{\cos(\theta_0 + u_s(t)(90° - \theta_0)/100)}{\cos(\theta_0)} \quad (1)$$

with the shutter command being limited to, $0 \le u_s(t) \le 100$ and $\theta_0 = 25°$. The controller of the shutter is able to move the blades to the target angle in less than $0.2s$.

B. Temperature model of the sample

An energy balance is used to model the temperature of the sample, such as the one made in [1]. The samples can have different shapes and sizes, but a circular shape with a diameter of $2cm$ and a height of $2mm$ can be considered a typical sample size. The temperature of the sample, $T_s(t)$ [K] is described (approximated) by

$$\frac{dT_s(t)}{dt} = -\alpha_1[T_s^4(t) - T_b^4(t)] - \alpha_2[T_s(t) - T_e(t)] \quad (2)$$

$$-A_{cool}(t) + \alpha_3 G_s(t)s_{fs}(u_s(t)) .$$

T_b [K] represents the temperature of the "enviroment" that contributes to losses by radiation and T_e represents the temperature of the surrounding air that contributes to losses by convection. The factors α_1 , α_2 and α_3 represent the process parameters, they are defined by

$$\alpha_1 = \frac{\epsilon(T_s)\sigma A_{sr}}{C_p(T_s)m}; \quad \alpha_2 = \frac{h_{conv}(T_s, T_e)A_{sc}}{C_p(T_s)m}; \quad \alpha_3 = \frac{\alpha_s A_{si}g_f}{C_p(T_s)m} . \quad (3)$$

and are identified using data collected from the process as shown in in fig. 4 (SiC sample) and in fig. 5 (Stainless Steel sample), where the shutter was commanded manually to change the temperature. The term $A_{cool}(t)$ represents the effect of active cooling using air flow that is calibrated by selecting a constant air pressure. The $A_{cool}(t)$ term is considered as a disturbance that the temperature controller acting on the shutter aperture must compensate, if needed.

In order to perform the process identification, $G_s(.)$ (available sun power) is recorded and the active cooling ($A_{cool}(t)$) is not applied.

The parameters in (3) are described in Table I.

TABLE I

THERMAL MODEL PARAMETERS

| Parameter : Description |
| --- |
| $\rho \ [kgm^{-3}]$: Density of the material |
| $C_p \ [Jkg^{-1}K^{-1}]$: Material Specific Heat |
| $m \ [kg]$: Mass of the sample |
| ϵ : Emissivity of the material |
| $\sigma \ [Wm^{-2}K^{-4}]$: Stefan-Boltzmann const. |
| $A_{sr} \ [m^2]$: Sample's loss radiation area |
| $A_{sc} \ [m^2]$: Sample's convection area |
| $A_{si} \ [m^2]$: Sample's incident area |
| $L_c \ [m]$: Characteristic length |
| $h_{conv} \ [Wm^{-2}K^{-1}]$: Convection factor |
| α_s : Sample's solar absorption factor |
| g_f : Furnace gain |
| $G_s \ [W/m^2]$: Max. Solar Flux |
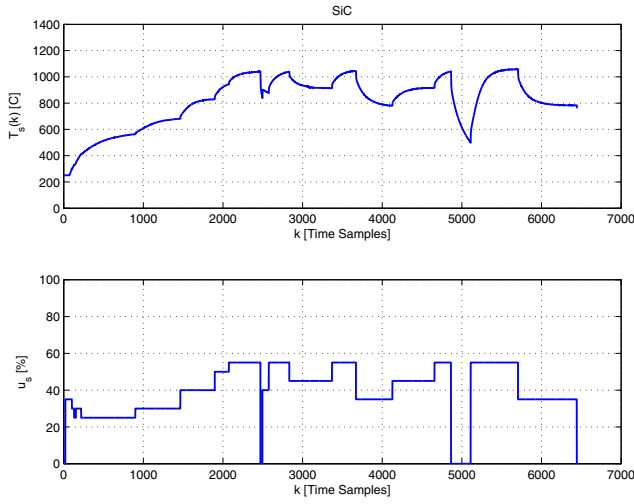
Fig. 4. Data collected from the solar furnace with a SiC sample, by manually adjusting the shutter. The material sample temperature is shown at the top and the manipulated variable is shown at the bottom. The solar power was almost constant during the experiment ($900W/m^2$).

III. OFF-LINE IDENTIFICATION OF THE TEMPERATURE MODEL

If a new material must be tested, there is an initial lack of information about its thermal properties (C_p, ϵ, α_s are unknown), and the parameters α_1, α_2 and α_3 that enter in equation of the temperature cannot be computed. As a consequence, if a first controller is used to track the temperature reference profile with a small error, then there is a risk that the sample will be melt due to temperature overshoots.

To solve the problem, data from the process, for temperatures below the material melting point, must be collected. This can be done by performing open loop tests, where the shutter is adjusted by an human operator or, a proportional controller can be used. In this case the human operator can adjust the controller gain by "small increments".

In order to identify the model parameters it is assumed that α_1, α_2 and α_3 are constant. Sampled data is used but the
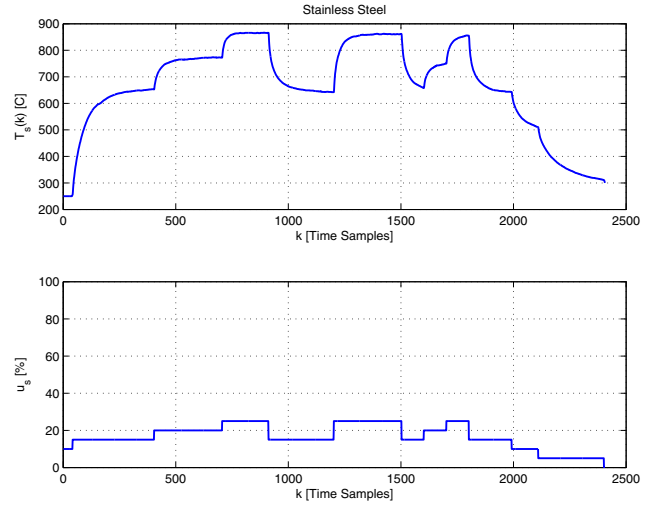

Fig. 5. Data collected from the solar furnace with a stainless steel sample, by manually adjusting the shutter. The material sample temperature is shown at the top and the manipulated variable is shown at the bottom. The solar power was almost constant during the experiment ($950W/m^2$).

noise generated by computing the numerical time derivative of $T_s(.)$ must be attenuated. To tackle above the problem, the following signals are defined, $\zeta_1(t) = [T_s^4(t) - T_e^4(t)]$, $\zeta_2(t) = [T_s(t) - T_e(t)]$ and $\zeta_3(t) = u_r(t) = G_s(t)s_{fs}(u_s(t))$ and a stable low-pass filter $O(s) = a/(s+a)$ with unitary static gain is applied to eq. (2), yielding

$$\frac{as}{(s+a)}T_s(s) = -\alpha_1 \frac{a\zeta_1(s)}{(s+a)} - \alpha_2 \frac{a\zeta_2(s)}{(s+a)} + \alpha_3 \frac{a\zeta_3(s)}{(s+a)} . \tag{4}$$

Parameter $a > 0$ is selected based on the level of noise present on $T_s(.)$ and also on the dynamics of the process. The general rule is to select the filter to be much faster than the temperature dynamics. It follows that (4) admits the continuous time representation,

$$\zeta_{f0}(t) = -\alpha_1 \zeta_{f1}(t) - \alpha_2 \zeta_{f2}(t) + \alpha_3 \zeta_{f3}(t) \tag{5}$$

with

$$\zeta_{f0}(t) = a(T_s(t) - T_{sf}(t)) \tag{6}$$

$$\frac{dT_{sf}(t)}{dt} = -aT_{sf}(t) + aT_s(t) \tag{7}$$

$$\frac{d\zeta_{f1}(t)}{dt} = -a\zeta_{f1}(t) + a\zeta_1(t) \tag{8}$$

$$\frac{d\zeta_{f2}(t)}{dt} = -a\zeta_{f2}(t) + a\zeta_2(t) \tag{9}$$

$$\frac{d\zeta_{f3}(t)}{dt} = -a\zeta_{f3}(t) + a\zeta_3(t) . \tag{10}$$

In order to solve these dynamic equations in discrete time, the first order hold (FOH) method is applied using the sampling time $h = 0.5s$. The estimation of parameters α_1, α_2 and α_3 are computed using the Least Mean Square (LMS) method with discrete time signals $\zeta_{f0}[t]$, $\zeta_{f1}[t]$, $\zeta_{f2}[t]$, $\zeta_{f3}[t]$.
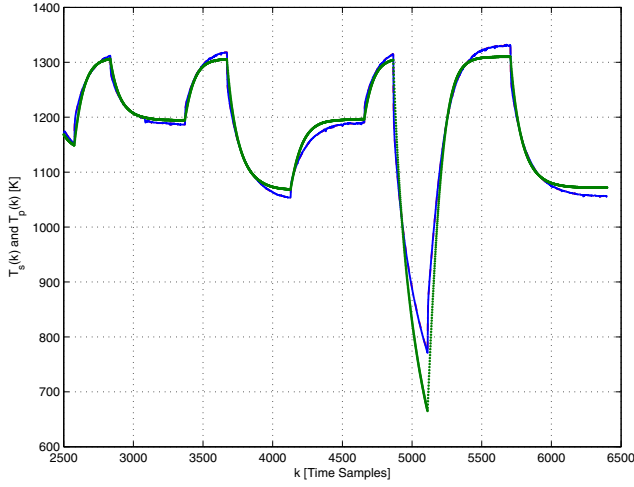
Considering (5) and the data at each time sample, it

Fig. 6. Off-line model identification of a SiC sample, data from fig.(4). The sample temperature $T_s(t)$ (blue colour) and the one-step ahead prediction are very similar. The model output with the initial state set to $T_s[2500]$ is shown in green colour. In both cases model output gives a good approximation of the process dynamics.
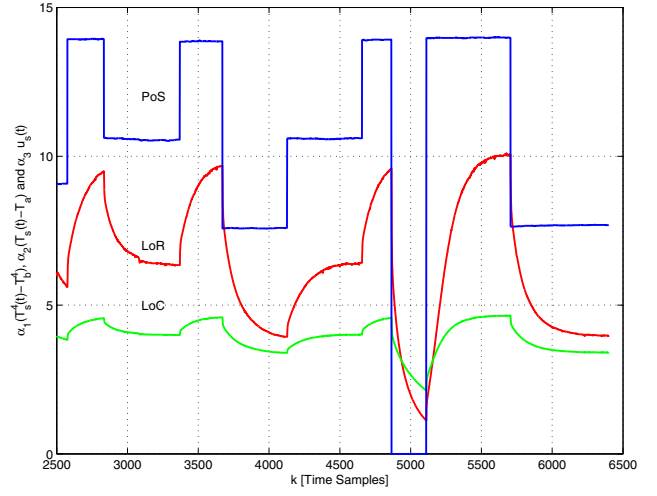

Fig. 7. Comparing the contribution of each term of temperature model dynamics in the SiC sample. LoC - Loss by Convection, LoR - Loss by Radiation, PoS - Power absorption

follows that,

$$
\begin{bmatrix} y[t] \\ y[t-h] \\ \cdots \\ y[t-nh] \end{bmatrix} = \begin{bmatrix} \zeta_{f1}[t] & \zeta_{f2}[t] & \zeta_{f3}[t] \\ \zeta_{f1}[t-h] & \zeta_{f2}[t-h] & \zeta_{f3}[t-h] \\ \cdots & \cdots & \cdots \\ \zeta_{f1}[t-nh] & \zeta_{f2}[t-nh] & \zeta_{f3}[t-nh] \end{bmatrix} \begin{bmatrix} \alpha_1 \\ \alpha_2 \\ \alpha_3 \end{bmatrix},
$$

(11)

that can be represented by $Y = \Phi\alpha$. The parameters are obtained from

$$
\alpha = (\Phi^T\Phi)^{-1}\Phi Y \tag{12}
$$

if the matrix $\Phi^T\Phi$ has inverse, this can be obtained using an excitation signal that has an adequate spectrum. In this work input steps are used. Note that in the present problem there is a huge difference between the values of $\zeta_{f1}[t]$ $\zeta_{f2}[t]$ $\zeta_{f3}[t]$, that are related to $T^4(.)$, $T(.)$, and $G_s(t)s_{fs}(u_s(t))$. This can cause numerical problems. To mitigate this problem the matrix Φ must be scaled by a diagonal matrix such that $Y = \Phi\Lambda\alpha_L$, with $\alpha_L = \Lambda^{-1}\alpha$.

The results of the off-line identification corresponding to a time window of fig. 4 are shown on fig. 6 where the sample temperature $T_s(t)$ (blue colour) and the one-step ahead prediction are very similar. The model output with the initial state set to $T_s[400]$ is shown in green colour. In both cases model output are good approximations of the process dynamics.

The scaling matrix was selected as $diag(\Lambda) = [2.0 \times 10^{-11}, 1.0 \times 10^{-2}, 1.0 \times 10^{-1}]$, the estimates of $\bar{\alpha}_1$, $\bar{\alpha}_2$ and $\bar{\alpha}_3$ are respectively, 3.213×10^{-12}, 4.5×10^{-2}, 3.20×10^{-2}.

Other important aspect that is provided by the model, is the quantification of the relation between the energy loss by radiation described by the term $\bar{\alpha}_1[T_s^4(t) - T_e^4(t)]$, that is nonlinear, and the term corresponding to energy loss by convection $\bar{\alpha}_2[T_s(t) - T_e(t)]$, that has a linear contribution to the temperature dynamics. The comparison is presented on fig. 7, from which it can be concluded that the nonlinear term dominates for temperatures higher than $1000K$. Below
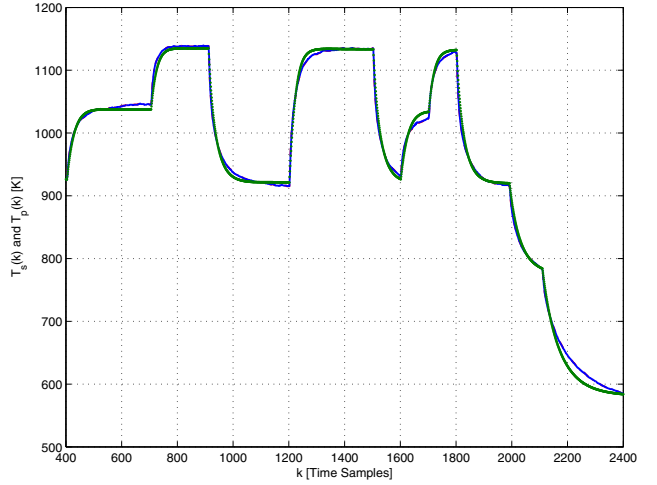

Fig. 8. Off-line model identification. Sample temperature $T_s(t)$ (blue colour) and the one-step ahead prediction are very similar. The model output with the initial state set to $T_s[400]$ is shown in green colour. In both cases model output gives a good approximation of the process dynamics.

this temperature value the energy loss by convection have a bigger contribution to the temperature dynamics.

The off-line model identification results of the stainless steel sample are shown in the figures fig. 8 and 9 where the the parameter estimates $\bar{\alpha}_1$, $\bar{\alpha}_2$ and $\bar{\alpha}_3$ are respectively, 1.590×10^{-11}, 1.581×10^{-2}, 2.608×10^{-1}.

IV. CONTROL LAW DESIGN

The proposed approach to design a controller is based on the definition of a virtual control input $u_r(t)$ such that $u_r(t) = G_s(t)s_{fs}(u_s(t))$. The aim is to impose $u_r(.)$ and to invert the nonlinearity such that $u_s(.)$ is computed and applied to the process input, note that $s_{fs}()$ is known and $G_s(t)$ is measured. Additionally, the proposed control will be based on the concept of exact linearization.
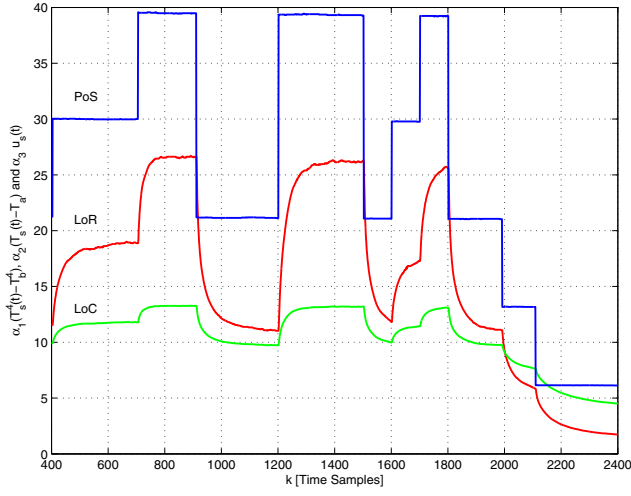
Fig. 9. Comparing the contribution of each term of temperature model dynamics. LoC - Loss by Convection, LoR - Loss by Radiation, PoS - Power absorption
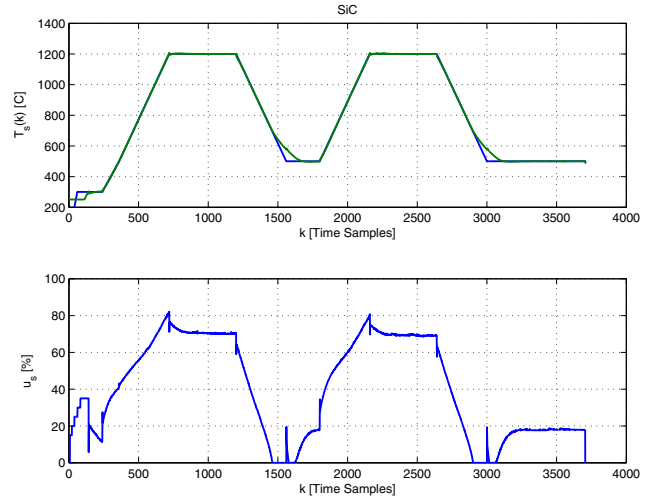

Fig. 10. Exp1: Temperature control of a SiC sample with the exact linearization coupled with a PI controller. During this experiment the sun power was almost constant $G_s(.) \approx 925 W/m^2$.

Define

$$e_s(t) \triangleq T_R(t) - T_s(t) , \tag{13}$$

where $T_R(t)$ represents the temperature reference and define the tracking error dynamics $\dot{e}_s(t) \triangleq \dot{T}_R(t) - \dot{T}_s(t)$, that can be written as

$$
\begin{aligned}
\dot{e}_s(t) &= \dot{T}_R(t) + \alpha_1[(T_R(t) - e_s(t))^4 - T_e^4(t)] \\
&+ \alpha_2[T_R(t) - e_s(t) - T_e(t)] - \alpha_3 u_r(t) .
\end{aligned} \tag{14}
$$

Expanding the nonlinear term $(T_R(t) - e_s(t))^4$ as $T_R^4(t) - 4T_R^3(t)e_s(t) + 6T_R^2(t)e_s^2(t) - 4T_R(t)e_s^3(t) + e^4(t)$ and assuming that $e_s(t)$ is small enough such that $(T_R(t) - e_s(t))^4 \approx T_R^4(t) - 4T_R^3(t)e_s(t)$, then (14) can be approximated by

$$
\begin{aligned}
\dot{e}_s(t) &= -[\alpha_1 4 T_R^3(t) + \alpha_2]e_s(t) + \dot{T}_R(t) + \alpha_1[T_R^4(t) - T_e^4(t)] \\
&+ \alpha_2[T_R(t) - T_e(t)] - \alpha_3 u_r(t) .
\end{aligned} \tag{15}
$$

Having the estimates $\hat{\alpha}_i$ of the process parameters α_i and estimates of the error bounds, such that $\alpha_i = \hat{\alpha}_i + \Delta\alpha_i$, the control signal is defined as $u_r(t) = \overline{u}_r(t) + \delta_r(t)$ with

$$\overline{u}_r(t) = \frac{\dot{T}_r + \hat{\alpha}_1(T_R^4(t) - T_0^4) + \hat{\alpha}_2(T_R(t) - T_e)}{\hat{\alpha}_3} . \tag{16}$$

where the term $\overline{u}_r(t)$ is used to cancel the nonlinear thermal dynamics. The dynamics of the tracking error can now be written as

$$
\dot{e}_s(t) = \frac{\Delta\alpha_3}{\hat{\alpha}_3}\dot{T}_R(t) + (\Delta\alpha_1 + \hat{\alpha}_1\frac{\Delta\alpha_3}{\hat{\alpha}_3})(T_s^4(t) - T_e^4(t)) +
$$
$$
\tag{17}
$$
$$
+ (\Delta\alpha_2 + \hat{\alpha}_2\frac{\Delta\alpha_3}{\hat{\alpha}_3})(T_s(t) - T_e(t)) - \alpha_3\delta_r(t) .
$$

The input $\delta_r(t)$ is used to compensate small parameter errors. Defining $\delta_r() = K_l/\hat{\alpha}_3(e_s(t) + K_p \int(e_s(\tau)d\tau)$ and considering that the $\Delta\alpha_i$ are small, the dynamics of the tracking error can be written as

$$\dot{e}_s(t) = -\frac{\alpha_3}{\hat{\alpha}_3}K_l(e_s(t) + K_i \int_0^t (e_s(\tau)d\tau) . \tag{18}$$

The parameters of the PI controller can now be selected such the the dynamics of the tracking error (18) is stable. Note that the terms of (17) that depend on $\Delta\alpha_i$ can be evaluated for the temperature reference profile and bounds can be computed and used to evaluate the robustness of the controller. A possible algorithm to select the PI controller parameters is to imposed a real double pole on the tracking error dynamics, where $K_i = 0.25 * K_l$. A discrete time version of the controller equations is implemented with a small sampling time compared with the time constant of the process. That provides a good approximation of the continuous time controller.

V. PRACTICAL EVALUATION OF THE CONTROL LAW

Figure 10 shows the results obtained during an experiment using the exact linearization with the PI controller. The PI controller gains are $K_l = 0.2$ and $K_i = 0.05$. The sun power was almost constant $G_s(.) \approx 925 W/m^2$.

From fig. 10, it can be concluded that a good temperature tracking is obtained when the temperature reference increases or during time intervals where the reference signal is constant. But when the reference decreases, energy loss by radiation and by natural convection do not allow a good tracking, the rate of energy loss is not adequate. To address this situation, active cooling (air flow - forced convection) is employed to decrease the temperature of the sample. This is presented in the fig. 11, where the air flow is applied from the beginning of the experiment and the $G_s(t) \approx 900 W/m^2$.

This action can be considered as a disturbance that the controller compensates by selecting an higher shutter aperture to apply more power on the sample that compensated the cooling action of the air flow.

An alternative approach is to apply the cooling action when if fact is needed, that is, during the temperature reference decrease. This is illustrated in fig. 12, where a
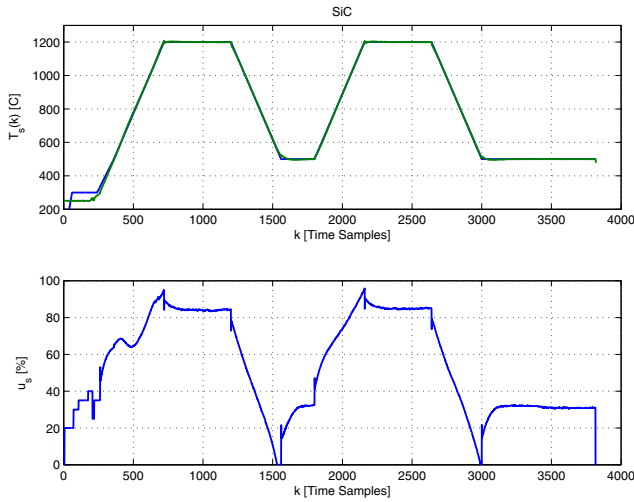
Fig. 11. Exp2: Using active cooling (air flow) from the beginning of the experiment to improve the temperature tracking during the decrease of the reference ($G_s(.) \approx 900W/m^2$).

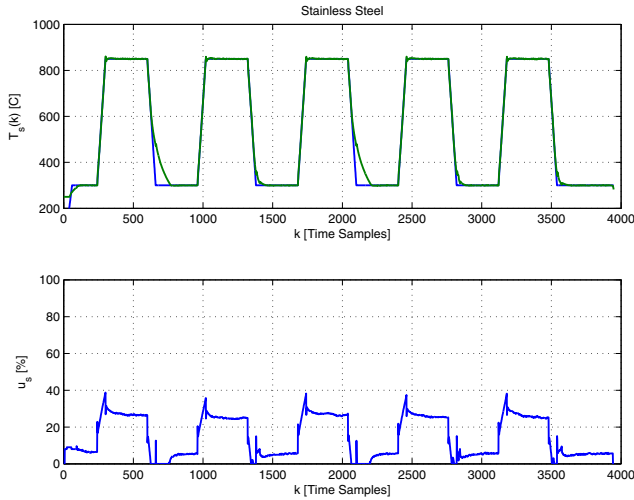Fig. 13. Exp3: Sun power during experiment 3 corresponding to the results shown in fig.(12).

Fig. 12. Exp3: Using active cooling (air flow), to improve the reference temperature tracking, of a stainless steel sample, during the second, fourth and fifth reference cycles (reference decrease).

stainless steel sample was used. The model parameters were obtained from the data presented in fig. 5. The active cooling (air flow) is applied during the second, fourth and fifth reference cycles (reference decrease) and that improves the temperature reference tracking.

In this case the sun power has a lower value and is not constant, fig. 13, but its effect is compensated by the controller, that has the gains $K_l = 0.5$ and $K_i = 0.125$.

VI. CONCLUSION

This paper describes the design of a control system for solar furnaces to perform cycling temperature stress tests.

The process dynamics accounts for the contribution of losses by radiation and by convection and solar energy absorption. Data collected from the process is used with
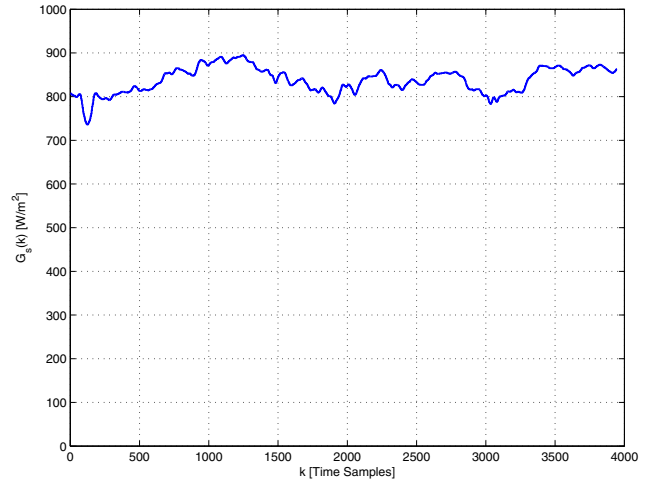
an off-line model identification method to characterize the temperature dynamics. This methodology avoids the use of online adaptation mechanisms that may cause stability problems during stress test. The control methodology is based on the exact linearization coupled with a PI to compensate model parameter uncertainty. Experiment test results show that the proposed methodology with active cooling improves the temperature reference tracking.

REFERENCES

[1] M. Berenguel, E. Camacho, F. Garcia-Martin, and F. Rubio, "Temperature control of a solar furnace," *IEEE Control Systems*, vol. 19(1), pp. 8–24, 1999.
[2] B. A. Costa and J. Lemos, "Singular perturbation stability conditions for adaptive control of a solar furnace with actuator dynamics," *European Control Conference 2009 Budapest Hungary*, 2009.
[3] ——, "Predictive adaptive temperature control in a solar furnace for material stress tests," *IEEE Multi-conference on Systems and Control 2012 Dubrovnik Croatia*, 2012.
[4] B. A. Costa and J. M. Lemos, "Optimal control of the temperature in a solar furnace," *Optimal Control Applications and Methods*, 2014.
[5] B. A. Costa and J. Lemos, "Temperature control of a solar furnace with exact linearization and off-line identification," *CONTROLO2014 Proceedings of the 11th Portuguese Conference on Automatic Control*, vol. 321, pp. 321–330, 2014.
[6] M. Beschi, M. Berenguel, A. Visioli, and L. Yebra, "Constrained control strategies for disturbance rejection in a solar furnaces," *Control Engineering Practice*, vol. 21, no. 10, pp. 1410 – 1421, 2013.
[7] M. Beschi, M. Berenguel, A. Visioli, J. L. Guzmn, and L. J. Yebra, "Implementation of feedback linearization {GPC} control for a solar furnace," *Journal of Process Control*, vol. 23, no. 10, pp. 1545 – 1554, 2013.
[8] ——, "On reduction of control effort in feedback linearization {GPC} strategy applied to a solar furnace," *Optimal Control Applications and Methods*, 2015.
[9] B. A. Costa and J. M. Lemos, "Control of a solar furnace using mpc with integral action," *Submitted to 11th IFAC Symposium on Dynamics and Control of Process Systems*, 2016.